Indian Journal of Pure & Applied Physics
Vol. 55, February 2017, pp. 155-162

# Generation and diagnostics of atmospheric pressure dielectric barrier discharge in argon/air

R Shrestha[a,b]*, D P Subedi[a], R B Tyata[a,c] & C S Wong[d]

[a]Department of Natural Science, Kathmandu University, Kathmandu 6250, Nepal
[b]Department of Physics, Nepal Banepa Polytechnic College, Banepa 2, Kavre, Nepal
[c]Department of Electrical, Khwopa College of Engineering, Bhaktapur 44800, Nepal
[d]Plasma Technology Research Centre, Physics Department, University of Malaya, Kuala Lumpur, Malaysia 50603

*Received 23 November 2014; revised 25 October 2015; accepted 5 December 2016*

In this paper, a technique for the determination of electron temperatures and electron densities in atmospheric pressure argon/air discharge by the analysis of optical emission spectra (OES) is reported. The discharge is produced using a high voltage (0-20 kV) power supply operating at a frequency of 27 kHz in parallel electrode system, with glass as dielectric. The dielectric layers covering the electrodes act as current limiters and prevent the transition to an arc discharge. Optical emission spectra in the range of 300 nm to 850 nm have been recorded for the discharge with different inter electrode gap keeping electric field constant. Electron temperature $T_e$ and electron density $n_e$ have been estimated from electrical and optical methods. Electron density has been calculated using power balance method. The optical methods are related with line intensity ratio from the relative intensities of Ar-I and Ar-II lines in Argon plasma. The electron density calculated by using line intensity ratio method has been compared with the electron density calculated by stark broadening method. The effect of dielectric thickness on plasma parameters has also been studied and it has been found that $T_e$ and $n_e$ increase as thickness of dielectric decrease for same inter electrode distance and applied voltage.

**Keywords:** Optical emission spectra, DBD, Electron temperature, Electron density

## 1 Introduction

In recent years, the non-equilibrium plasma at atmospheric pressure is arousing keen interest among industrial plasma processing researchers[1]. Atmospheric pressure non equilibrium plasma has been widely applied in material processing such as surface modification of textiles or organic materials for improvement of hydrophilicity and hydrophobicity, new material preparation such as carbon nanotubes[2,3], element analysis, environmental protection, toxic gas removal, plasma sterilization for medical application, and medical tools in dermatological treatment, disposal of industrial waste etc[4-6]. Atmospheric pressure plasma surface treatment has been studied at 50 Hz as well as at higher frequency discharges[7,8]. This type of plasma does not require vacuum system and they are suitable for continuous in-line processing. The low-temperature atmospheric plasma includes corona discharge, dielectric barrier discharge, micro-hollow cathode discharge, one-atmospheric-uniform-glow discharge plasma and surface wave discharge[9]. An atmospheric pressure, capacitively coupled discharge plasma fed with argon gas had been examined by Balcon *et al*[10]. It was found that parallel plate reactor could be operated in homogeneous glow mode and filamentary mode with variation of applied voltage and frequency.

The plasma discharge in atmospheric pressure dielectric barrier discharges shows filamentary and homogeneous (diffuse type) discharge, which depends upon the experimental conditions such as gas type, shape and size of the electrode, electrode gap, dielectric materials and applied voltage waveform[11,12]. In fact the applied voltage waveform plays a key role in the discharge efficiency.

In this paper, the investigation on a dielectric barrier discharge using sinusoidal waveform in atmospheric pressure operated in both filamentary and glow modes is presented. In the atmospheric pressure DBD discharge, the *in-situ* diagnostic is not possible due to small inter-electrode distance and passive diagnostics become important. So, the present work includes electrical and optical characterization of atmospheric pressure DBD dielectric barrier discharge plasma with single dielectric barrier glass between two conducting electrodes. The electrical analysis of discharge has been performed using an equivalent electrical circuit model.

*Corresponding author (E-mail: rajendra.ts2002@gmail.com)

## 2 Experimental Setup

The schematic diagram of experimental arrangement is shown in Fig. 1. The electrodes are made up of two brass discs, 10 mm thick and 60 mm in diameter. A glass plate with thickness of 1.2 to 2 mm is used as dielectric barrier between the two brass electrodes. A high voltage ac source with amplitude variable from 0 to 20 kV and frequency variable from 10 to 30 kHz was used to power the discharge through a current limiting resistor of 10 kΩ. The whole apparatus is enclosed in a cylindrical chamber and argon is passed into it. The argon flow rate was maintained at 2 l/min. The argon DBD plasma is generated with different electrode gaps of 1 to 3 mm between the parallel plate electrodes.

## 3 Electrical Characterizations

The optical and electrical properties of the DBD plasma depend on the permittivity and thickness of the dielectric material used. The ratio of relative permittivity to barrier thickness, $\varepsilon_r/d$ has significant influence on the electron density, electron temperature and density of reactive species of the plasma[13,14].

In Fig. 2, $V_o$ is the input voltage, $I_o$ is the total current in the circuit, $C_g$ is the capacitance of inter electrode gap and $C_d$ is the capacitance of dielectric barrier which can be determined by using the Eq. (1) and the charge transferred into gas discharge per cycle of applied voltage across conducting electrodes can be determined[14] from Eq. (2).

$$C_d = \frac{\varepsilon_r \varepsilon_o A}{d} \quad \ldots (1)$$

$$Q = 4\left[C_d\left(V_p - V_b\right) - C_g V_b\right] \quad \ldots (2)$$

Here $V_p$ and $V_b$ are the applied voltage and breakdown voltage, respectively.

The energy dissipated per cycle is given by:

$$E = QV_b = 4[C_d(V_p - V_b) - C_g V_b]V_b \quad \ldots (3)$$

and the power dissipated per cycle is given by:

$$P = \frac{E}{T} = \text{FE} \quad \ldots (4)$$

where $f = \frac{1}{T}$ is the frequency of the voltage applied.

In the electrical method to estimate the electron density by power balance method, the total energy lost by the electron in the plasma is assumed to be balanced by the input power[15,16], hence:

$$n_e = \frac{P}{2AeV_b E_{lost}} \quad \ldots (5)$$

where $P = VI$ is the input power, $A$ is the areas of electrodes, $e$ is the charge on the electron, and $V_b$ is the Bohm velocity.

## 4 Optical Emission Spectroscopy

In the present experiment, mixture of air and argon is used as a working gas for the generation of atmospheric pressure DBD. The amount of energy

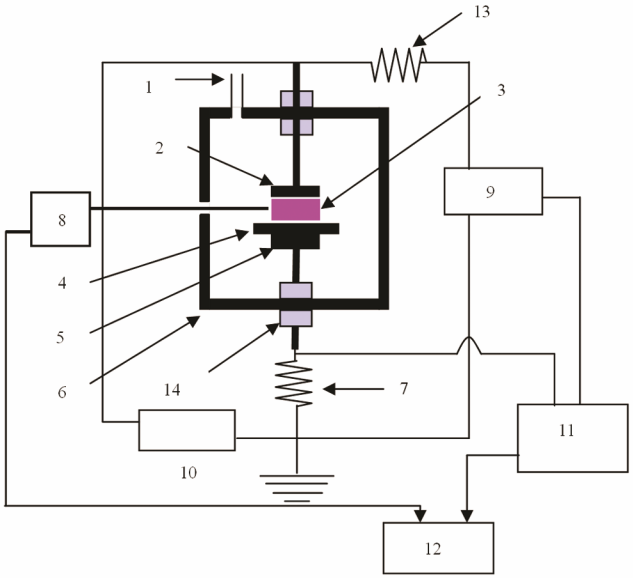


Fig. 1 – Schematic diagram of experimental arrangement consisting of gas inlet (1), parallel disc electrodes (2), discharge (3), glass plate (4), grounded electrode (5), enclosing chamber (6), resistance 10 k Ω (7), linear array spectrometer VS140 (8), voltage probe (9), ac power supply (10), oscilloscope (11), computer (12), resistance 10 MΩ (13), Teflon screw (14)

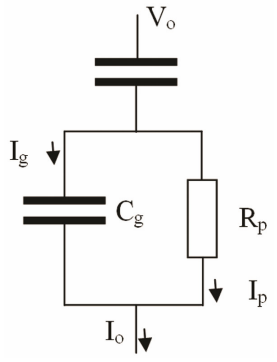


Fig. 2 – Electrical equivalent circuit of DBD with single dielectric barrier $C_d$

required to generate and sustain the discharge depends on the inter electrode distance. At a fixed inter electrode distance and atmospheric pressure, when the energy reaches to certain breakdown value, the discharge starts with discrete filamentary distribution on the dielectric barrier surface and becomes consistent with rise in applied voltage. In the discharge plasma, the electrons gain energy from the applied electric field and undergo inelastic collision with neutral plasma species. As a sequence of the inelastic collisional process, some of the neutral plasma species gain sufficient excitation energies and jump into higher energy states, which decay back to lower energy states by emitting the photon of characteristic wavelengths.

The optical emission spectroscopy (OES) technique used for determination of plasma parameters is based on the measurement of relative intensities of two or four spectral lines from two consecutive ionic species[16]. The intensity of spectral lines depends on $kT_e$ and proportional to the population density of excited states. Hence $kT_e$ can be determined by using the Boltzmann plot[17,18] where:

$$KT_e \frac{E_2 - E_1}{\log\left[\frac{I_1}{I_2}\frac{\lambda_1}{\lambda_2}\frac{g_2}{g_1}\frac{A_2}{A_1}\right]} \quad \ldots (6)$$

In Eq. (6), indices 1 and 2 refer to the first and second spectral lines. $I$ is the measured intensity of selected spectral lines, $k$ is the Boltzmann constant, $E$ is the excited state energy, $g$ is the statistical weight, and $A$ is the transition probability.

The Boltzmann plot method is valid if the discharge plasma under study is in complete local thermodynamic equilibrium (LTE)[19]. But in our experiment it is no likely that LTE will hold due to low plasma density. Therefore, this method may not be used for the exact determination of $kT_e$ and $n_e$. It can provide us estimated values of the plasma parameters under varying working condition of discharge plasma. In the spectrum, the Argon lines are observed in the range of 300 to 900 nm and $kT_e$ is determined by selecting two argon spectral lines. The intensities of these spectral lines are obtained from the observed spectrum. The values of $E$, $g$ and $A$ for the selected lines are taken from the NIST atomic spectra data sheet. Using all these values in Eq. (6), the $kT_e$ can easily be determined as a function of applied voltage, inter electrode gap and gas flow rate. The electron density $n_e$ can be determined by using the relative intensity of atomic and ionic spectral lines in Boltzman-Saha equation[10], where $I_1$ is the intensity of the *Ar-I* line, $I_2$ is the intensity of *Ar-II* line, $\lambda_1, \lambda_2$ are wavelengths, $A_1, A_2$ are the transition probabilities, and $g_1, g_2$ are the statistical weights of levels (neutral) and (ionized), respectively:

$$n_e = 2\left(\frac{I_1}{I_2}\right)\left(\frac{\lambda_1}{\lambda_2}\right)\left(\frac{A_2}{A_1}\right)\left(\frac{g_2}{g_1}\right)\left[\frac{2\pi m_e kT_e}{h_2}\right]^{\frac{3}{2}} Exp\left[-\frac{E_1 - E_2 + E_i}{KT_e}\right] \quad \ldots (7)$$

## 5 Measurement of Electron Density by Stark Broadening Method

Stark broadening is caused by the Coulomb interaction between the radiator (in this case argon atom) and the electron or ion present in the plasma. The stark broadening appearing due to collision of charged particles is the primary mechanism influencing the width of Ar emission lines. The stark broadening function has the Lorenzian profile. The electron density is related to the width of stark broadening by the following expression[20]:

$$\Delta\lambda_{Stark} = 2\omega\left[\frac{n_e}{10^{16}}\right] + 3.5\alpha\left[\frac{n_e}{10^{16}}\right]^{\frac{1}{4}} \times \left[1 - \frac{3}{4}N_D^{-1/3}\right]\omega\left[\frac{n_e}{10^{16}}\right] \quad \ldots (8)$$

where, $\omega$ is the electron impact width parameter, $\alpha$ is the ion broadening parameter, $n_e$ is the electron concentration and $N_D$ is the number of particle in Debye sphere.

The first term in Eq. (8) refers to the broadening due to the electron contribution and the second term to the ion broadening contribution. The ionic term can be neglected because the ion broadening in Ar is very small[21]. Thus Eq. (8) can be reduced to a simple form:

$$\Delta\lambda_{stark} = 2\omega\frac{n_e}{10^{16}} \quad \ldots (9)$$

Both $\omega$ and $\alpha$ are tabulated for different temperature in[21]. Hence, $n_e$ can be expressed as:

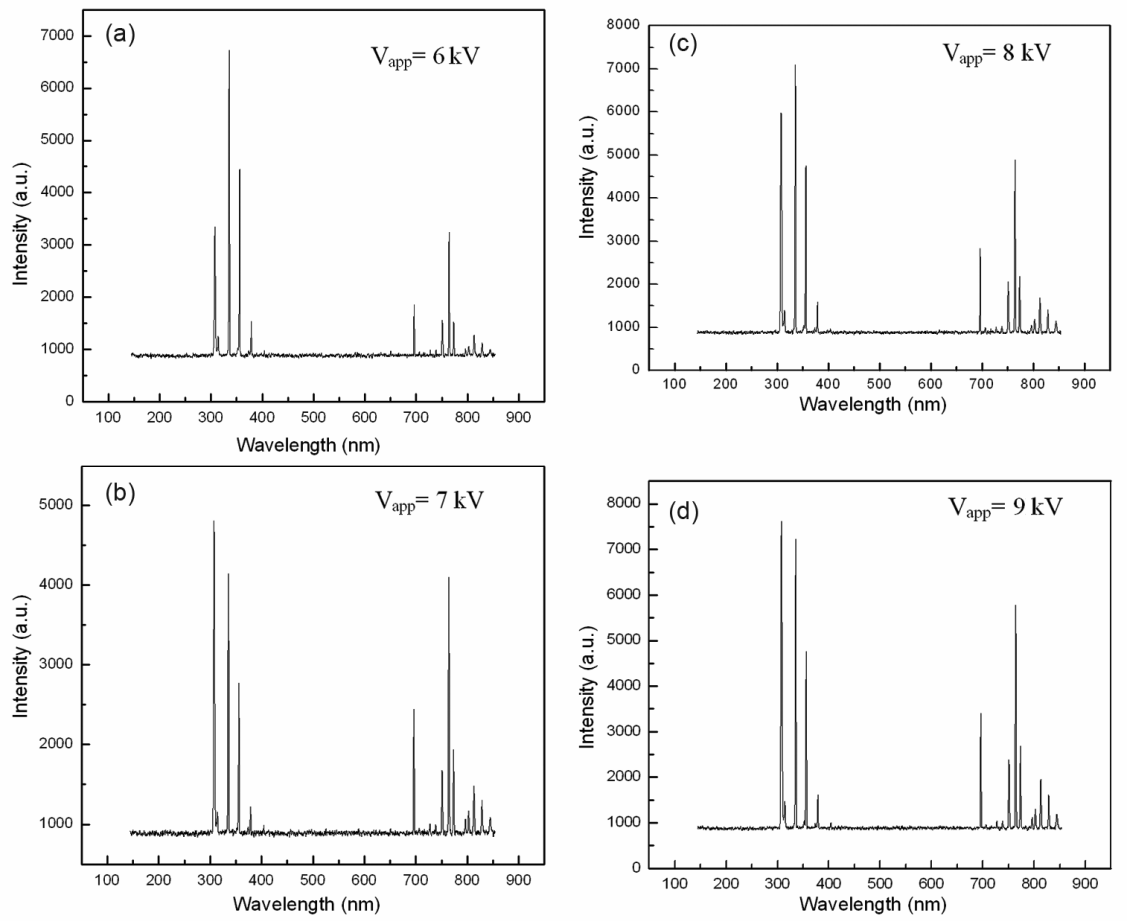


Fig. 3 – Emission spectrum recorded at different applied voltage for determination of $T_e$ and $n_e$

$$n_e = \left[\frac{\Delta\lambda_{stark}}{2\times10^{-11}}\right]^{\frac{3}{2}} \quad \ldots(10)$$

## 6 Results and Discussion

The calculation of electron temperature was done by using Eq. (6) and electron density was calculated by using Eqs (5), (7) and (10). The plasma parameters depend on applied voltage and inter electrode distance because other are kept constant. The optical emission spectra of DBD generated at applied voltages of 6 kV, 7 kV, 8 kV and 9 kV are shown in Fig. 3(a), (b), (c) and (d), respectively. Similarly, Figs 4 and 5 shows the intensities of OH radical (307 nm) and Ar-I line (696.54 nm), respectively, as a function of applied voltage. It is evident from Figs 4 and 5 that intensities of both lines are proportional to the applied voltage. This can be attributed to the fact that the concentration of active species: (OH radical) and excited species of Ar increase with the increase in applied voltage and the intensity of the

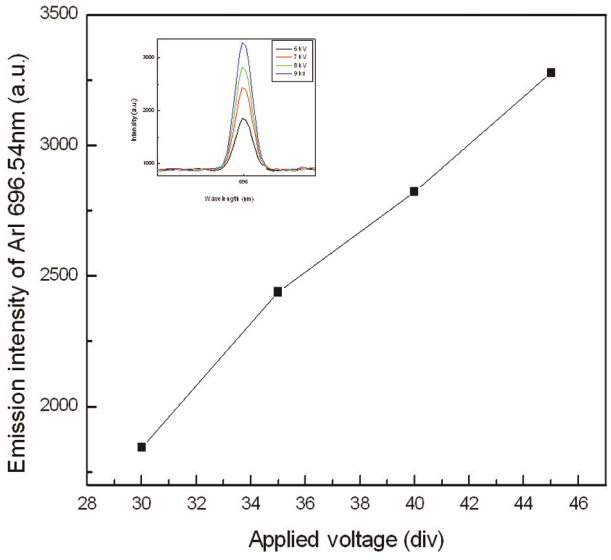


Fig. 4 – Emission intensity of ArI 696.54 nm as function of applied voltage

emission line is proportional to the concentration of these species. Figure 6(a–d) shows the spectra used to determine the FWHM for the Ar-I line (696.54 nm) for the DBD generated at different voltages ranging from 6 kV-9 kV. The spectroscopic results for $T_e$ and $n_e$ as as function of applied voltage are shown in Figs 7 and 8. From Fig. 7, it is clear that the electron temperature increases with the increase in applied voltage This result is in agreement with the results reported earlier[11,14].

Similarly, from Fig. 8 it is evident that the electron density also increases with the applied voltage. Figure 9 depicts the variation of electron density with electron temperature. Figure 10(a–e) shows current and voltage waveforms of the discharge using dielectric of

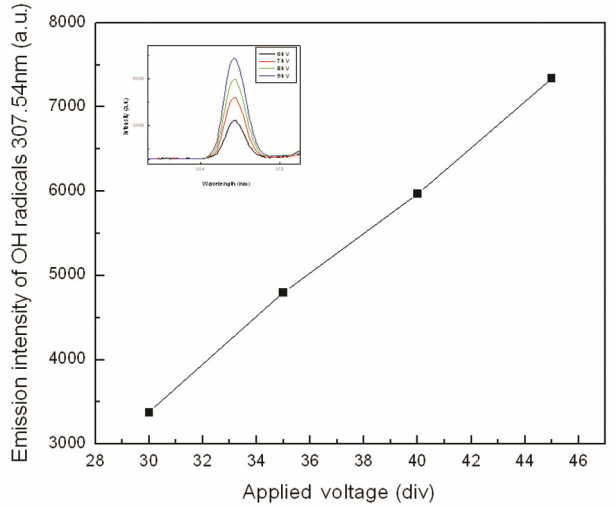


Fig. 5 – Emission intensity of OH radicals 307.54 nm as function of applied voltage

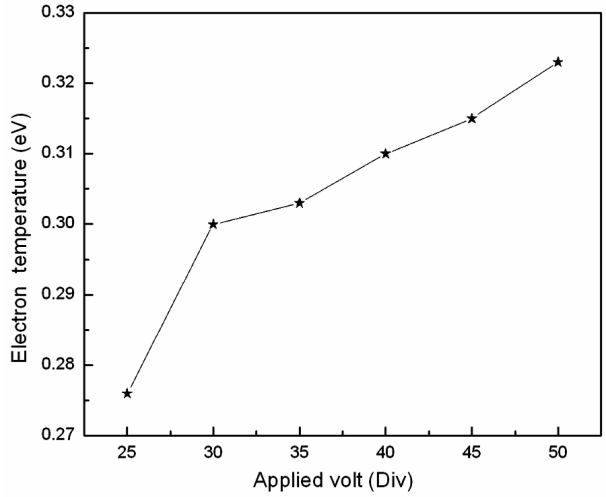


Fig. 7 – Electron temperature as function of applied voltage

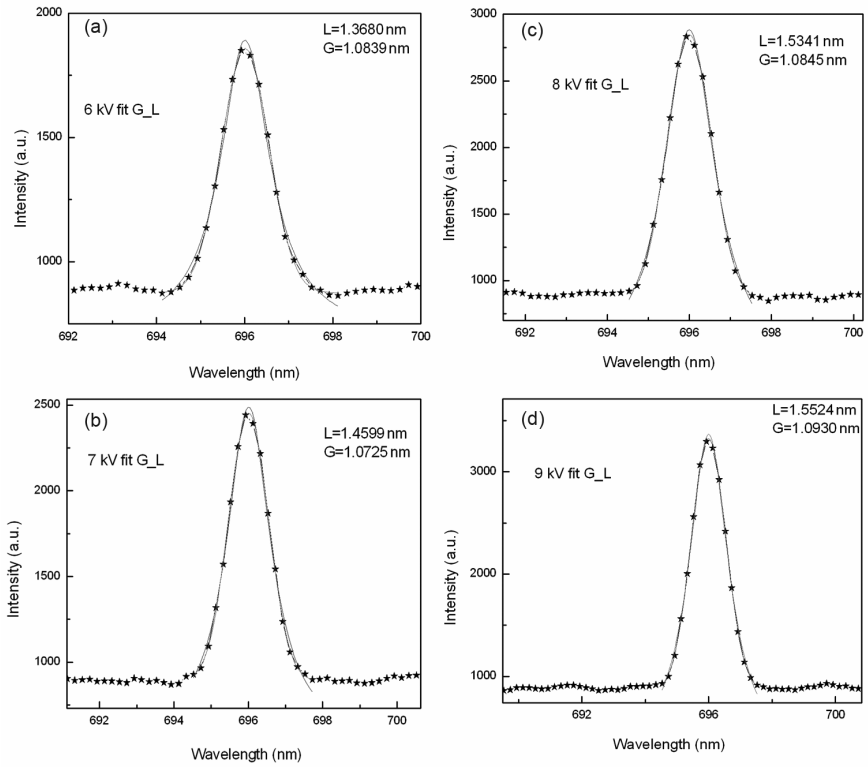


Fig. 6 –Spectra for determination of full width at half maxima FWHM

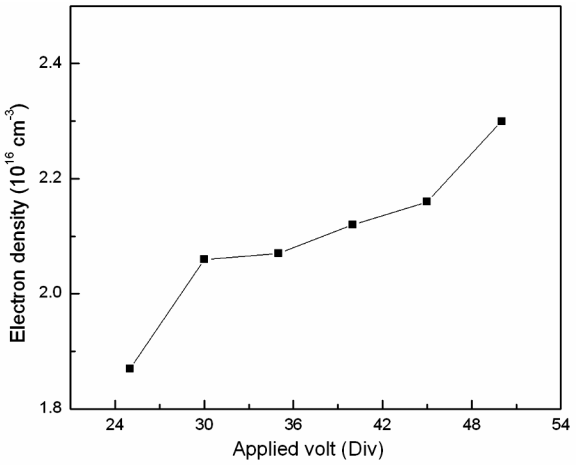


Fig. 8 – Electron density as function of applied voltage

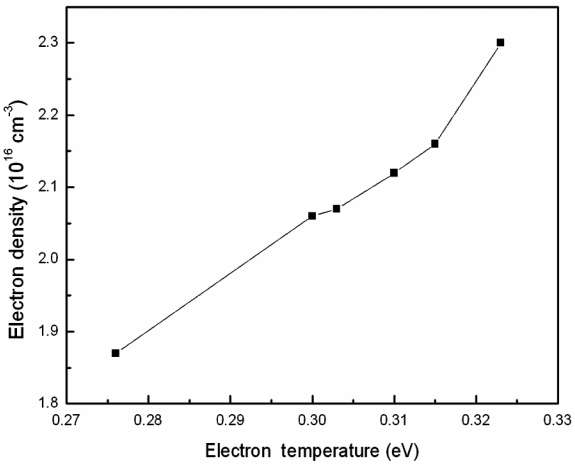


Fig. 9 – Electron density vs electron temperature in DBD

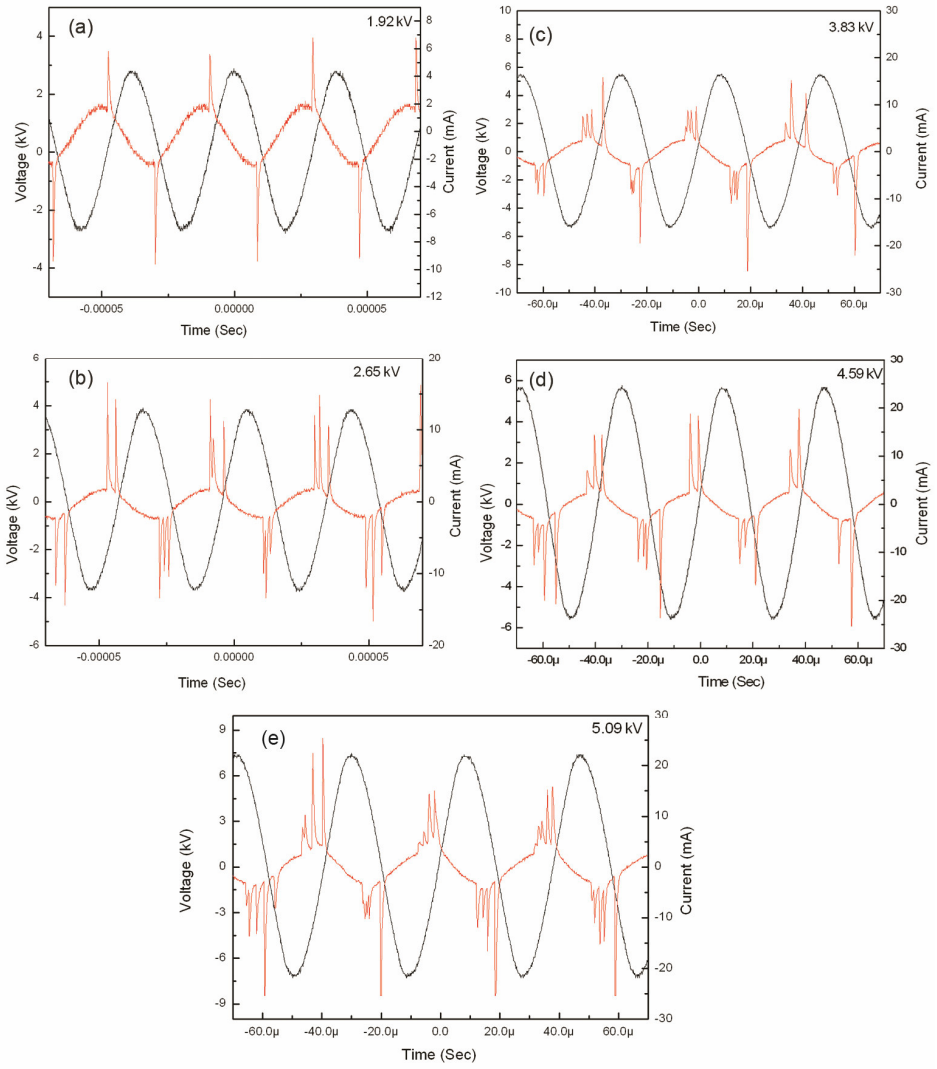


Fig.10 – Current and voltage wave form of discharge using dielectric of thickness 1.1 mm and inter-electrode distance 2 mm

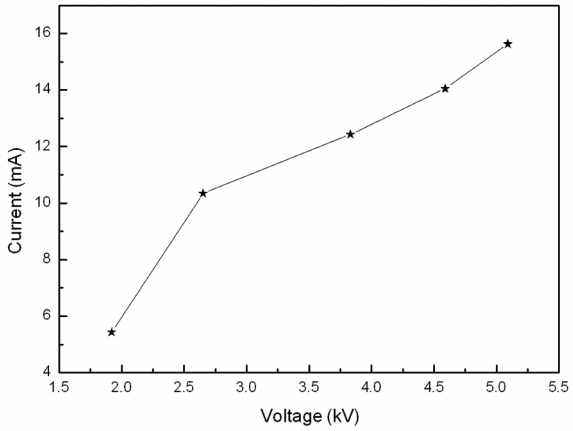


Fig. 11 – Discharge current as function of applied voltage in discharge using glass dielectric of thickness 1.1 mm

Table 1 – Values of discharge current, power consumption and electron density measured at various values of applied voltage

| Applied voltage (kV) | Current (mA) | Power consumption (W) (From *IV* product) | Power consumption (W) (From Lissajous figure) | Electron density ($10^{13} \times cm^{-3}$) |
|---|---|---|---|---|
| 1.92 | 5.43 | 10.42 | 13 | 1.86 |
| 2.65 | 10.30 | 27.29 | 30 | 4.89 |
| 3.83 | 12.40 | 47.49 | 52 | 8.50 |
| 4.59 | 14.05 | 64.49 | 69 | 11.5 |
| 5.09 | 15.63 | 79.56 | 85 | 14.2 |

thickness 1.1 mm and inter-electrode distance of 2 mm. In Fig. 10(a), single current peak in each half cycle indicates that the discharge is in glow mode. From Fig. 10(b–e), it is clear that the numbers of spikes are strongly influenced by the applied voltage.

The spike in the current waveform represents the micro discharge in the plasma. Figure 11 shows the variation of current in discharge with applied voltage. From Fig. 12, it is clear that the electron temperature increases with the increase in applied voltage in atmospheric pressure dielectric barrier discharge. Values of discharge current, power consumption and electron density measured at various values of applied voltage are summarized in Table 1. It shows that electron density increases with increase in applied power to the discharge. The discharge current and discharge power are compared for different thickness of dielectrics and the variation trends of both are shown in Figs 13 and 14. For thinner dielectric barrier, the observed behavior might be due the higher secondary electron emission coefficient of the glass. Figure 15 shows the variation of electron density in DBD using different dielectric thickness and it can be seen that $n_e$ increases as thickness of dielectric decreases.

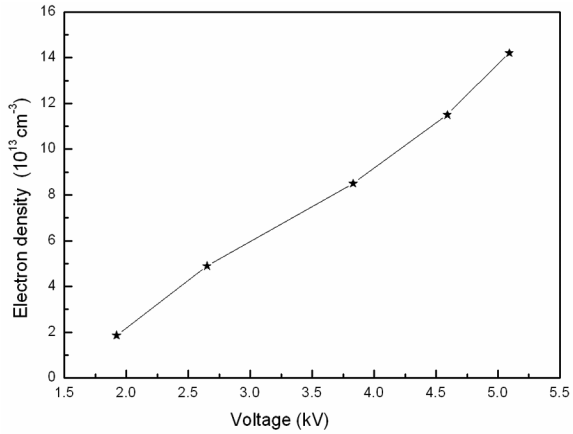


Fig. 12 – Electron density as function of applied voltage in discharge using glass dielectric of thickness 1.1 mm

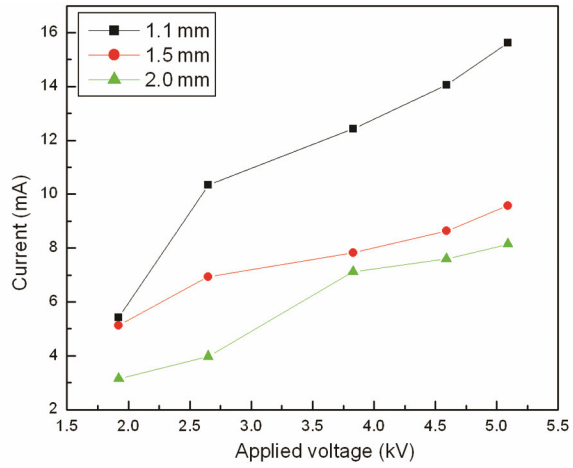


Fig. 13 – Comparison of discharge current for different thickness of dielectric glass

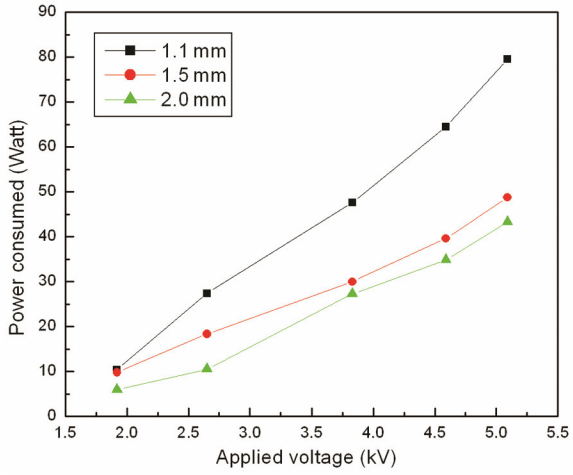


Fig. 14 – Variational trend of discharge power with applied voltage

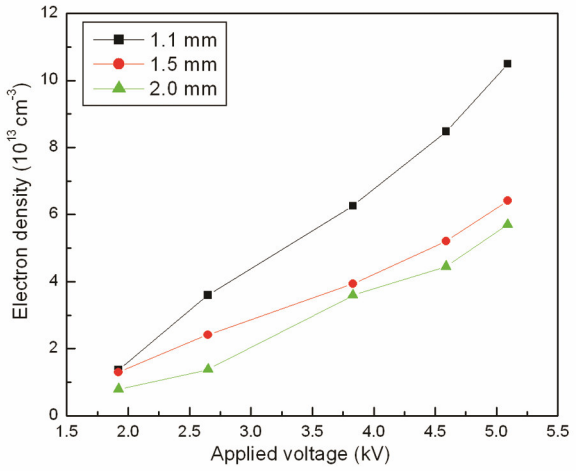


Fig. 15 – Electron density as the function of applied voltage for different thickness of dielectric

## 7 Conclusions

Atmospheric pressure dielectric barrier discharge system with single dielectric barrier layer between disc electrodes is generated by the application of high voltage ac source of variable frequency (up to 30 kHz) and voltage in the range of 0 to 20 kV. The glass dielectric barrier of thickness 1.1 mm, 1.5 mm and 1.95 mm are used for DBD generation independently. The spectroscopic and electrical characterization of atmospheric DBD plasma are carried out and the discharge power, electron density and electron temperature are determined as function of applied voltage and dielectric barrier thickness. It is observed that all DBD parameters increase with increase in applied voltage and decreases with increase in dielectric thickness. From the electrical properties of the discharge, it is clear that glow discharge can be obtained by using thinner dielectric barrier but for very thin dielectric barrier layer, DBD can go into the arc region.

## Acknowledgement

This work was supported by National Academy of Sciences and Technology (NAST). The participation C S Wong in this project is being supported by University of Malaya research grant RP008-13AFR.

## Reference

1 Kogelschatz U, *Plasma Chem Plasma Process*, 23 (2003) 0272.
2 Becker K H, Kogelschatz U, Schoenbach K H & Barker R J, *IOP, University of reading*, *Berkshir*, 2005.
3 Nozaki T & Okazaki K, *Plasma Process Polym*, 5 (2008) 300.
4 Laroussi M, *IEEE Trans Plasma Sci,* 36 (2008) 1612.
5 Zhang Q, Sun P, Feng H, Wang R & Liang Y, *J Appl Phys*, 111 (2012) 123305.
6 Kuchenbecker M, Bibinov N, Kaemlimg A, Wandke D, Awakowicz P & Viol W, *J Phys D Appl Phys*, 42 ( 2009) 045212.
7 Fang Z, Qiu X, Qiu Y & Kuff E, *IEEE Trans Plasma Sci*, 34 (2006).
8 Chua P K, Chen J Y, Wang L P & Huang N, *Mater Sci Eng R*, 36 (2002) 143.
9 Okazaki S, Kagoma M, Uehara M & Kimura Y, *J Phys D Appl Phys*, 26 (1993) 889.
10 Balcon N, Aanesland A & Boswell R, *Plasma Sources Sci Technol*, 16 (2007) 217.
11 Belostotskiy G S, Ouk T, Donnelly V M, Economou D J & Sadeghi N, *J Appl Phys*, 107 (2010) 053305.
12 Osawa N & Yoshioka Y, *IEEE Trans Plasma Sci*, 40 (2011).
13 Mariotti D, Shimizu Y, Sasaki T & Koshizaki N, *J Appl Phys*, 101 (2007) 013307.
14 Nazl M Y, Ghaffar A, Rehman N U, Sahid S A & Shukrullah S, *Int J Eng Technol*, 12 (2012).
15 Shrestha R, Tyata R B & Subedi D P, *Himalayan Phys*, 4 (2013).
16 Shrestha R, Tyata R B & Subedi D P, *Kathmandu University J Sci Eng Technol*, 8 (2012) 37.
17 Subedi D P, Tyata R B, Shrestha R & Wong C S, *AIP Conf Proc*, 1588 (2014) 103.
18 Tyata R B, Subedi D P, Shrestha R & Wong C S, *Pramana J Phys*, 80 (2013) 507.
19 Unnikrishnan V K, Alti K, KarthaV B, Santhosh C, Gupta G P & Suri B M, *Pramana J Phys*,74 (2010) 983.
20 Ohno N, Razzak M A, Ukai H, Takamura S & Uesugi Y, *Plasma Fusion Res*, 1 (2006) 028 (9 pp).
21 Dong L F, Ran J X & Mao Z G, *Appl Phys Lett*, (2005) 8616150.